

Dispersivity-saturation relationship in a lab-scale soil column

Master Thesis

L. van Broekhuizen

Author: Ludo van Broekhuizen

Student number: 3847594

Supervisor: dr. Amir Raouf

Second supervisor: dr. Mojtaba Ghareh Mahmoodlu

Earth Surface and Water

Faculty of Geosciences

Utrecht University, the Netherlands

Abstract

Solute transport through porous media is affected by variations in pore-flow velocity which cause meandering of flow paths. This causes the solute to spread in both longitudinal and transversal directions. This spreading is defined as hydrodynamic dispersion in the advection-dispersion equation (ADE). Dispersivity is a property of a porous medium that is linearly related to the hydrodynamic dispersion through pore-water velocity. In this study the relation between dispersivity and soil water content is investigated by conducting solute displacement experiments in a soil column under saturated and unsaturated conditions.

A pulse of a CaCl_2 tracer solute was injected into a soil column and the concentration was measured at three depths along the column using electrical conductivity sensors. The resulting breakthrough curves (BTCs) were analyzed to determine the dispersivity, using the solution of the ADE by the CXTFIT2 software code.

Results show the dispersivity values that were an order of magnitude larger for the unsaturated soils than for the saturated soils. This demonstrates the large dependency of dispersivity on soil water content. However, the results did not allow a clear relation to be determined. This is caused by a lack of data points and a lack of a mobile-immobile transport model, which could probably describe solute transport in unsaturated soils more accurately than the ADE.

Contents

1	Introduction	1
2	Theory	1
3	Materials and Methods.....	4
3.1	Saturated Hydraulic Conductivity Measurements	4
3.2	Preparation of the Soil Column	5
3.3	Multistep Outflow Method	6
3.4	HYDRUS-1D Model.....	6
3.4.1	General Model Setup.....	7
3.4.2	Direct Model.....	8
3.4.3	Indirect Model.....	8
3.5	Analysis of the Soil Water Retention Curve.....	9
3.6	Column Experiments	10
3.6.1	Saturated Experiment	10
3.6.2	Unsaturated Experiment	12
3.7	Permittivity Measurements as a Proxy for Concentration.....	13
3.8	Parameter Estimation.....	14
4	Results and Discussion	14
4.1	Unsaturated Water Flow	14
4.2	Breakthrough Curves and Parameter Estimation.....	15
5	Conclusions.....	18
6	References.....	20
	Appendices	I
	Appendix A	I
	Appendix B	III

List of Figures

1 - Schematic of the experimental setup for measuring saturated hydraulic conductivity.....	5
2 - Graphs resulting from the multistep outflow experiment.	7
3 - Schematic of the experimental setup for the saturated column experiment.	11
4 - Schematic of the experimental setup for the unsaturated column experiment.	12
5 - Relation between measured concentration and measured volumetric water content in a saturated experiment	13
6 - Graph of volumetric water content profile during unit-gradient flow for both unsaturated experiments.....	14
7 - Observed and fitted breakthrough curves at all three measured depths with concentrations expressed relative to the injected concentration:.....	15
8 - Dispersivity as a function of volumetric water content, for saturated and unsaturated conditions in both experiments	17
9 - All breakthrough curves of the first experiment plotted together and separate.....	I
10 - All breakthrough curves of the second experiment plotted together and separate.....	II

List of Tables

1 - Advection-dispersion equation (ADE) parameter estimations obtained from the breakthrough curves for saturated and unsaturated flow conditions in both experiments.	16
2 - Soil column measurements	III
3 - Packed soil column data for both experiments.....	III

1 Introduction

The unsaturated zone (vadose zone) extends from the ground surface to the groundwater. It stores water which is available to the biosphere through root uptake, for example, as well as water which serves as a medium for transport between the ground surface and groundwater reserves below. The unsaturated zone has been a recipient of industrial and agricultural wastes at many locations in the past and present. These locations include, but are not limited to, industrial sites dumping wastes in surface waters, leaking chemical containers and fertilized crop fields. To predict the behavior of contaminants and nutrients in soils, it is necessary to understand solute transport processes in the unsaturated zone. This knowledge can then be used to schedule ground remediation operations, optimize agricultural production methods, and secure fresh-water supplies. Flow in the unsaturated zone has been the subject of many studies, mainly within soil science and geotechnical engineering. However, new objectives for modelling of unsaturated solute transport arise when considering growing concerns regarding geo-environmental problems. One of the objectives is linking macro-scale properties like solute dispersivity, effective diffusion and mass transfer coefficients to water-saturation and pore-sizes. There is a lack in knowledge about the underlying mechanisms controlling multiscale behavior. This leaves inconsistent experimental results unexplained, and a knowledge gap that is widely cited as the primary barrier to acceptable predictions.

When a solute travels through a porous medium, mechanical dispersion and molecular diffusion cause it to spread in the longitudinal direction as well as the transversal direction. Although the physical processes of mechanical and dispersion molecular diffusion are different, the resulting solute transport can be combined into one single spreading process, called hydrodynamic dispersion (Bear, 1972).

This study focusses on the relation between the degree of water saturation and the solute dispersivity. The objective is to get a better understanding of the relationship between these two parameters and, if possible, define a quantitative relationship. In order to achieve this, both saturated and unsaturated soil column experiments were performed in the laboratory to obtain information on macro-scale solute distribution during unsaturated flow. A CaCl_2 tracer solute was injected in a laboratory scale soil column and its concentration was measured to determine breakthrough curves (BTCs). Values for transport parameters were determined by analyzing these BTCs. A one-dimensional flow model has also been constructed using HYDRUS-1D to simulate the experiment.

2 Theory

The solute flux, J_s [$\text{ML}^{-2}\text{T}^{-1}$], is given by the sum of the convective flux and the hydrodynamic dispersive flux:

$$J_s = qC - \theta D \frac{\partial C}{\partial z} \quad (1)$$

Where q is the Darcy water flux [LT⁻¹], C is the solute concentration [ML⁻³], θ is the volumetric water content [-], D is the hydrodynamic dispersion coefficient [L²T⁻¹] and z is the spatial coordinate [L]. The one-dimensional transport equation for variably-saturated flow conditions is given by (Simůnek et al., 2013):

$$\frac{\partial(\theta C + \rho_b s)}{\partial t} = \frac{\partial}{\partial z} \left(\theta D \frac{\partial C}{\partial z} \right) - \frac{\partial(qC)}{\partial z} - \theta C \mu_w - \rho_b s \mu_s + \rho_b \gamma_s + \theta \gamma_w - r \quad (2)$$

where t is time [T], z is the spatial coordinate [L], C [ML⁻³] and s [-] are concentrations in the liquid and solid phases, respectively, ρ_b is the bulk density [ML⁻³], μ_w and μ_s are first-order degradation coefficients for the liquid and solid phases [T⁻¹], respectively, γ_w [ML⁻³T⁻¹] and γ_s [T⁻¹] are zero-order production coefficients for the liquid and solid phases, respectively, and r is a sink term for root solute uptake [ML⁻³T⁻¹].

Since this study uses a tracer solute to eliminate all factors other than advection and dispersion, the terms describing adsorption, decay and root water uptake can be eliminated and the equation becomes:

$$\frac{\partial(\theta C)}{\partial t} = \frac{\partial}{\partial z} \left(\theta D \frac{\partial C}{\partial z} \right) - \frac{\partial(qC)}{\partial z} \quad (3)$$

This is generally known as the advection-dispersion equation (ADE), which is the most suitable model for describing solute transport in porous media.

The hydrodynamic dispersion coefficient for saturated soils is given by (Bear, 1972):

$$D(v) = D_e + \alpha v^n \quad (4)$$

where D_e is the effective diffusion coefficient [L²T⁻¹] and the second term describes the mechanical dispersion, where α is the dispersivity [L], v is the pore-water velocity [LT⁻¹] (given by J_w/θ) and n is an empirical constant.

The Peclet number, P_e , is given by (Fried and Combarous, 1971):

$$P_e = \frac{vL}{D_e} \quad (5)$$

where L is the characteristic mixing length which, when dealing with homogeneous porous media, is the mean pore radius or soil particle radius [L].

As the Peclet number is defined as a ratio between advective transport and diffusive transport, it shows the significance of the two types of transport. As P_e increases, the influence of diffusion on the solute spreading process becomes smaller, to the point where it is negligible. If P_e values are between 5 and 20, or even higher, the effect of molecular diffusion on hydrodynamic dispersion

becomes negligible and the hydrodynamic dispersion is nearly linearly related to pore-water velocity (i.e., $n = 1$) when dealing with a nonaggregated sand soil or glass beads (Bear, 1972; Bolt, 1979). equation (4) can then be rewritten as:

$$\alpha = D/v \quad (6)$$

When the porous medium is not saturated, the hydrodynamic dispersion will be dependent on dispersivity and pore-water velocity as well as volumetric water content. The relation between hydrodynamic dispersion and volumetric water content is then a modified form of equation (4):

$$D(\theta, v) = D_e(\theta) + \alpha(\theta)v^n \quad (7)$$

In previous studies, larger dispersivity values have been linked to unsaturated soils than to saturated soils (Beven et al., 1993; Haga et al., 1999; Maciejewski, 1993; Maraqa et al., 1997; Raouf and Hassanizadeh, 2013; Toride et al., 2003; Bunsri et al., 2008). These relations have been based on either models, experiments or both. However, the results shown by these studies are not sufficiently coherent and do not represent sufficient data to draw a complete conclusion on the relation between the degree of saturation in a soil and the dispersivity. Some studies have shown the relation between hydrodynamic dispersion and volumetric water content to be linear (Maciejewski, 1993), where other studies have found other relations. For example, the dispersivity in any unsaturated soil, independent of the degree of water saturation, was found to be larger by a factor of 2, as compared to a the dispersivity in a saturated soil (Maraqa et al., 1997).

A large part of this study focusses on solute dispersion under unsaturated one-dimensional flow conditions. Fluid flow in unsaturated porous media is described by the Richards equation which, when the volumetric water content is used as an independent variable, is written as (Celia and Bouloutas, 1990):

$$\frac{\partial \theta}{\partial t} = \nabla \cdot K(h) \nabla h + \frac{\partial K}{\partial z} \quad (8)$$

where h is the pressure head [L] and $K(h)$ is the unsaturated hydraulic conductivity [LT^{-1}] given by:

$$K(h) = K_s K_r(h) \quad (9)$$

where K_s is the saturated hydraulic conductivity [LT^{-1}] and K_r is the relative hydraulic conductivity [-] (Šimůnek et al., 2012).

In the case of one-dimensional uniform flow, equation (8) can be simplified to:

$$\frac{\partial \theta}{\partial t} = \frac{\partial}{\partial z} \left(K(h) \frac{\partial h}{\partial z} \right) \quad (10)$$

In a steady state flow regime, where θ is constant along the entire depth of the soil column, $\partial\theta/\partial t$ in equation (10) is equal to zero. In order to achieve this, unit-gradient flow is needed, which implies that the matric potential gradient is zero in the entire column and the gravitational potential gradient is equal to one in the entire column. As the gravitational potential gradient is equal to one by definition, the experimental objective to induce a steady state flow regime with a constant θ with depth is met when the matric potential gradient is made to be zero across the column.

3 Materials and Methods

In this section, a detailed description of the modeling steps as well as the experimental steps will be presented. In short, the research has been carried out as follows:

First, the saturated hydraulic conductivity of the sand was measured. Then, the soil column was packed using the same sand and prepared for the experiments.

A direct HYDRUS-1D model was constructed to be used as a blueprint for the experiments and to estimate the duration of achieving unit-gradient flow from an initially saturated column.

An experiment known as the multistep outflow method (MOM) was conducted with the packed soil column. The results of the MOM were used as input for an indirect HYDRUS-1D model to obtain the Van Genuchten parameters in the soil water retention function. Together with previously obtained retention curve data, the Van Genuchten parameters were used as input for a retention curve model (RETC) to determine the relative hydraulic conductivity for the degree of saturation which was desired in the unsaturated column experiments. This value for the relative hydraulic conductivity was then used as an approximation of the constant water flux at the top of the unsaturated column experiments.

Then, both the saturated and unsaturated column experiments were carried out to observe BTCs. The BTCs were then analyzed using STANMOD.

3.1 Saturated Hydraulic Conductivity Measurements

The saturated hydraulic conductivity, K_s , of the sand was determined using the constant head method as was described by Reynolds et al. (2002). First, a small cylinder was packed with the experimental sand. A mesh filter was fitted at the bottom, holding the sand in place whilst allowing free flow of water. Then water was added to the cylinder to induce ponded infiltration with the ponded water at a constant height. Any surplus of water was drained by an outlet in the cylinder. The flow rate through the soil sample was then measured by collecting the outflowing water over a set period of time, in this case 120 seconds, and weighing it. The experimental setup is shown in Figure 1. The experiment was carried out triplicate and the results were averaged to reduce the

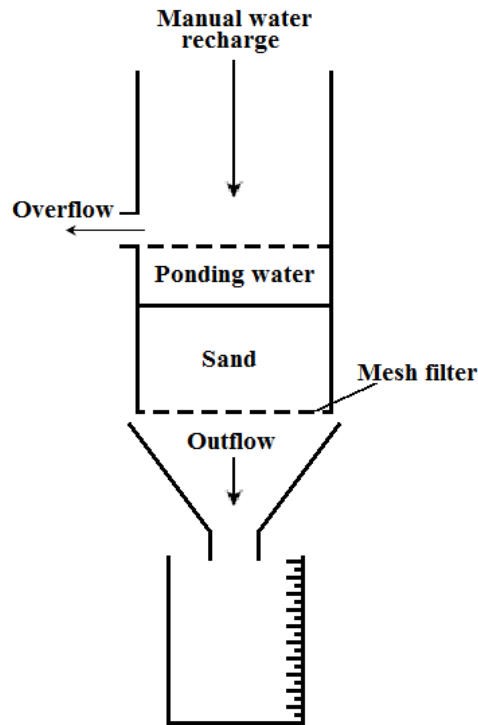


Figure 1 - Schematic of the experimental setup for measuring saturated hydraulic conductivity.

effects of measurement inconsistencies. The resulting measured K_s , was 69.1 m day^{-1} with the three data points within a margin of 2.2 m day^{-1} .

3.2 Preparation of the Soil Column

According to the definition that was stated by Folk and Ward (1957), the sand that was used for the experiments was very well sorted. The sand had a D50-value of 0.501 mm , and 95% of the grains had a diameter between 0.401 and 0.611 mm .

A column with an inner diameter of 9.5 cm and a length of 36.9 cm was filled with the sand in portions whilst each portion of sand was compacted before adding the next. In doing so, the degree of compaction was ensured to be virtually uniform across the length of the column. The resulting dry bulk densities of the two packed columns, ρ_b , were 1701 kg m^{-3} and 1629 kg m^{-3} , respectively. The soil was kept in place by a ceramic filter at the bottom of the column which allowed only water to pass through it, preventing leakage of sand and air. After the soil was compacted, three Decagon 5TE sensors were inserted horizontally into the column at their respective distances of 10.85 cm , 18.1 cm and 25.6 cm from the top of the column. Each 5TE sensor has three prongs that are inserted into the soil. Two of these prongs contain an electrode. Between the two electrodes electrical conductivity is measured by sending a small charge from one electrode to the other. The third prong measures the volumetric water content of the soil. Inserting the 5TE sensors and the tensiometers was done carefully to prevent disturbance of the soil structure. For the unsaturated experiments,

three tensiometers were installed at the same distances from the top of the column. The 5TE sensors and tensiometers were connected to a CR1000 Measurement and Control System data logger, manufactured by Campbell Scientific. The data logger was connected to a personal computer and to which it wrote its measuring data every minute. The 5TE sensors measured the temperature, volumetric water content and electrical conductivity. The tensiometers measured the water pressure. During the column preparation all relevant parameters were measured, such as weight, volume and length measurements. This data was needed to calculate the soil parameters and transport parameters.

3.3 Multistep Outflow Method

In order to obtain the soil hydraulic parameters of the soil in the column, the multistep outflow method (MOM), as described by Schelle et al. (2010), was used. These parameters include the residual water content, θ_r [-], the saturated water content, θ_s [-], parameter α in the Van Genuchten soil water retention function [L^{-1}], parameter n in the Van Genuchten soil water retention function [-], and the tortuosity, τ [-] (Van Genuchten, 1980).

The saturated soil column was connected to a hanging column to regulate the pressure head at the bottom of the column. The initial soil water pressure head was equal to zero at the bottom of the column. The column was then drained by decreasing the pressure head stepwise with 10 cm at a time. The pressure head steps for the column were 0, -10, -20 and -30 cm. With each step, water was drained from the column until equilibrium was reached. When equilibrium was reached the pressure head was decreased again. The cumulative bottom flux (outflow), Q (mL), was measured manually with an interval of one minute. The matric potential, h (cm), was measured by the three tensiometers and this data was also collected with a one-minute interval. The resulting graphs of the cumulative bottom flux and water potential are shown in Figure 2.

For the processing of the data an inverse solution of the HYDRUS-1D model was used. The cumulative bottom flux data as well as the tensiometer data was used as input, as well as the measurements of the column.

3.4 HYDRUS-1D Model

A model of the experimental soil column was made using HYDRUS-1D to simulate water flow through the column. This was done to simulate the water flow regime for the experiments and acquire an indication of the time it would take to reach unit gradient flow in the unsaturated

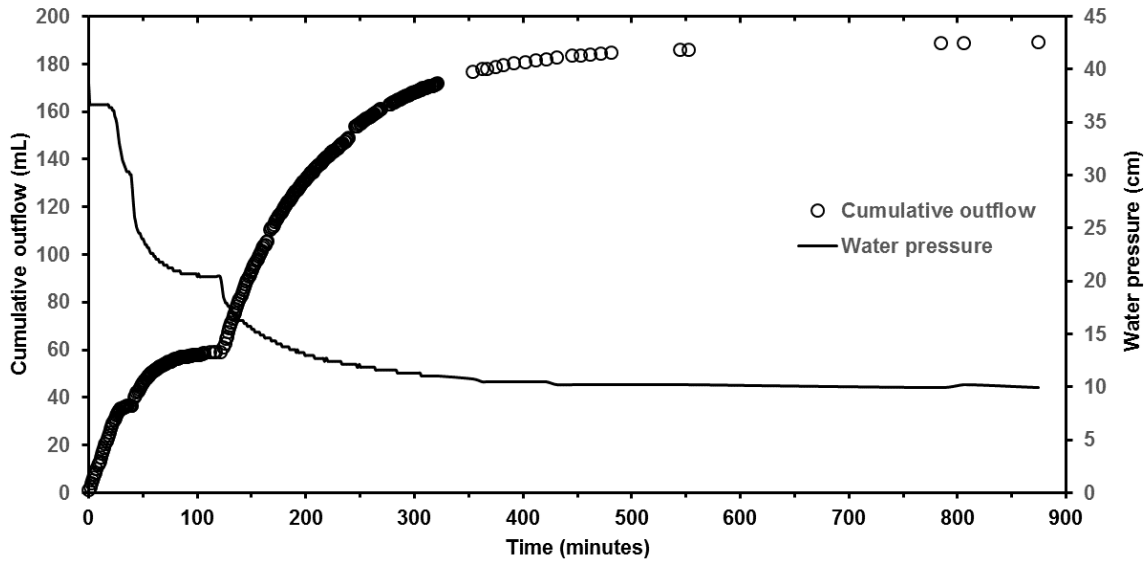


Figure 2 - Graphs resulting from the multistep outflow experiment.

experiments. Furthermore, the model was used to calculate an estimate of the Van Genuchten parameters in the soil water retention function.

The HYDRUS-1D code is a finite element model for simulating one-dimensional movement of water, heat and solutes in incompressible, variably saturated, porous media (Šimůnek et al., 2013). In this study HYDRUS-1D will only serve to calculate water movement. HYDRUS-1D numerically solves the Richards equation (equation 10) to simulate both saturated and unsaturated water flow.

3.4.1 General Model Setup

The HYDRUS-1D model was constructed to simulate water flow through a soil column which was described as a one-layered soil profile consisting of one soil material. The one-dimensional domain was 36 cm long and consisted of 1 node per centimeter, totaling at 37 nodes from 0 cm to 36 cm. The number of observation points that show up in the output data was set to five. These observation points were spread evenly across the domain of the model at 9 cm intervals. An overview of the model domain is shown in. The single porosity hydraulic model by Van Genuchten (1980) was used with no hysteresis. The sand classification values from the built-in soil catalog of HYUDRUS-1D were used as an initial estimate of the Van Genuchten parameters for the soil water retention function.

3.4.2 Direct Model

A direct simulation of the HYDRUS-1D model was carried out in order to simulate the water flow during the unsaturated experiment. Furthermore, the simulation was used to estimate the time it would take to achieve unit gradient flow from a saturated initial condition.

Boundary Conditions

The upper boundary condition for water flow was set to be a constant water flux and the lower boundary condition for water flow was set to a constant pressure head. This was done to simulate the constant water flux that was induced at the top of the column by the peristaltic pump and the hanging column that controlled the pressure head at the bottom of the column.

Initial Conditions

The initial conditions for the water content were expressed in pressure head. The entire column was saturated at the start of the experiment so the initial pressure head was set to zero. Only at the top and bottom of the column a different initial pressure head value was set. At the bottom the desired boundary condition for unit gradient flow was set as the initial condition, which would remain constant for the entire simulation. At the top of the column the initial pressure head value cannot be set to zero because the coding prevents the model to work if water flows towards a saturated cell. This would happen during the first time step because the constant water flux from the top of the column would then be directed towards the saturated top cell. In order to solve this, the pressure head value closest to zero that the model would accept was set as the initial condition.

3.4.3 Indirect Model

An indirect HYDRUS-1D model was constructed to simulate the MOM and obtain the hydraulic parameters of the soil through inverse modeling of the MOM data.

Boundary conditions

The upper boundary condition for water flow was defined as a constant flux with a value of zero, because in the MOM there is no flux at the upper boundary of the column. The lower boundary condition was set to be a pressure head which was variable over time. For this variable pressure head four steps are defined. These steps coincide, in terms of time and pressure head, with the pressure head steps that are taken in the experiment and are described earlier in the methods section.

Initial conditions

As was the case in the direct model, the initial conditions for the water content were expressed in pressure head. The entire column was saturated at the start of the experiment so the initial pressure was set to zero. The initial pressure head at the top of the column, as opposed to the initial pressure

head in the direct model, could be set to zero because there was no water flux from the top of the column.

Soil hydraulic parameters

All the soil hydraulic parameters that were mentioned in the Multistep outflow method section were fitted with the model. HYDRUS-1D contains a built-in soil parameter catalog. The sand-classification from this catalog was used to provide the initial estimates for fitting the parameters. For the saturated conductivity the value from the saturated conductivity measurements was used as the initial estimate.

Data for inverse solution

The data for the inverse solution consists of data pairs of time and cumulative bottom flux as well of data pairs of time and water pressure, which was obtained with the tensiometers. This was the data that was obtained with the MOM.

The resulting values for the Van Genuchten parameters that were obtained were then used for the inverse modeling of the soil water retention curve.

3.5 Analysis of the Soil Water Retention Curve

Prior to this research a soil water retention curve has been measured for the sand that is used in the experiments. This retention curve was used to determine the relative hydraulic conductivity for specific values of saturation. Hence, the retention curve data was analyzed using RETC, a code for quantifying the hydraulic functions of unsaturated soils.

The retention curve model for the relative conductivity, K_r , that was used is the Van Genuchten-Mualem model with limitations for the empirical shape factors m and n (Leij et al., 1989):

$$K_r = S_e^l [1 - (1 - S_e^{1/m})^m]^2 \quad (m = 1 - 1/n; 0 < m < 1) \quad (11)$$

where S_e is the reduced water content, denoted as $(\theta - \theta_r)/(\theta_s - \theta_r)$, and l is a model parameter, which commonly equated to 0.5.

The water flow parameters, or Van Genuchten parameters, that were used as input were the values obtained by inversely modeling the MOM with HYDRUS-1D. The water pressure-saturation data pairs from the retention curve were then used to fit a soil water retention curve to the data points, which resulted in values for the relative hydraulic conductivity for the sand soil in unsaturated conditions. The relative hydraulic conductivity is then multiplied by the saturated hydraulic conductivity as is shown in equation (9) to obtain the hydraulic conductivity for a specific saturation value. The resulting hydraulic conductivity values then serve as the water flux values for the pump in the unsaturated experiments.

These sequential measurement and modeling steps may influence the accuracy of the estimated hydraulic conductivity, so the hydraulic conductivity values may not have been entirely accurate. However, the hydraulic conductivity values that were calculated gave a rough estimate of the required pump rate in the unsaturated experiments and were therefore a good starting point before optimizing the pump rate.

3.6 Column Experiments

Prior to saturating the soil column, carbon dioxide was used to flush the soil column. Carbon dioxide is more soluble in water than atmospheric air. Therefore, the carbon dioxide that replaces the air will dissolve into the pore water and flow out of the column more rapidly than air bubbles. This way, the amount of air entrapment is minimized (Perret et al., 2000).

Then, after calibrating the peristaltic water pump, the column was connected to a water container. The column was saturated with deionized water, which was degassed by running argon gas through it. Saturating the column was done at a low flow rate from the bottom of the column. This was done to prevent air entrapment in the soil by fast flowing water.

The experiment was carried out twofold, i.e. the column was packed twice and after both packings the saturated and unsaturated experiments were carried out. During the experiment the electrical conductivity of the water in the column was measured at three locations. The electrical conductivity is a measure of the salt concentration in the water. The relationship between the soil electrical conductivity and the soil solute concentration for a constant θ is generally considered to be linear (Rhoades et al., 1989).

For the experiments a 0.02M concentration of CaCl_2 was used as the tracer solute. The concentration of 0.02M was low enough not to significantly influence fluid density and high enough to be detected by the electrical conductivity sensors. The transport processes that may affect the CaCl_2 solution are advection molecular diffusion and mechanical dispersion. The diffusion coefficient, D_e for this tracer has been calculated according to research by Ribeiro et al. (2008), which stated the following relationship based on diffusion coefficient measurements on CaCl_2 solutions:

$$D_e = a_0 + a_1 C + a_2 C^2 \quad (12)$$

where a_0 [L^2T^{-1}], a_1 [$(\text{L}^2\text{T}^{-1}) \text{molarity}^{-1}$], and a_2 [$(\text{L}^2\text{T}^{-1}) \text{molarity}^{-2}$] are empirical parameters which relate to the temperature of the CaCl_2 solution and C is the CaCl_2 molar concentration. The calculated value of D_e is $1.19 \times 10^{-9} \text{ m}^2 \text{ s}^{-1}$.

3.6.1 Saturated Experiment

A schematic of the saturated experimental setup is shown in Figure 3. During the saturated experiment the peristaltic pump was connected to the bottom of the column and therefore the water

flow direction was pointed upwards. Water flowing upwards prevented bubbles from being trapped in the column, which would prevent the column from becoming uniformly saturated. At the top of the column the water flowed out and was disposed in a waste container. The waste container was weighed before and after the experiment in order to determine the water flux during the experiment.

Before each experiment, the pump was turned on and a uniform steady flow regime was induced. When the desired flow velocity was established, the valve connecting the peristaltic pump to its water container was switched from using deionized water to using a salt tracer for a specified period of time and the data logger was switched on. After the specified amount of time had passed the valve was switched back to using the deionized water. The experiments kept running until the salt tracer was flushed by the deionized water in its entirety.

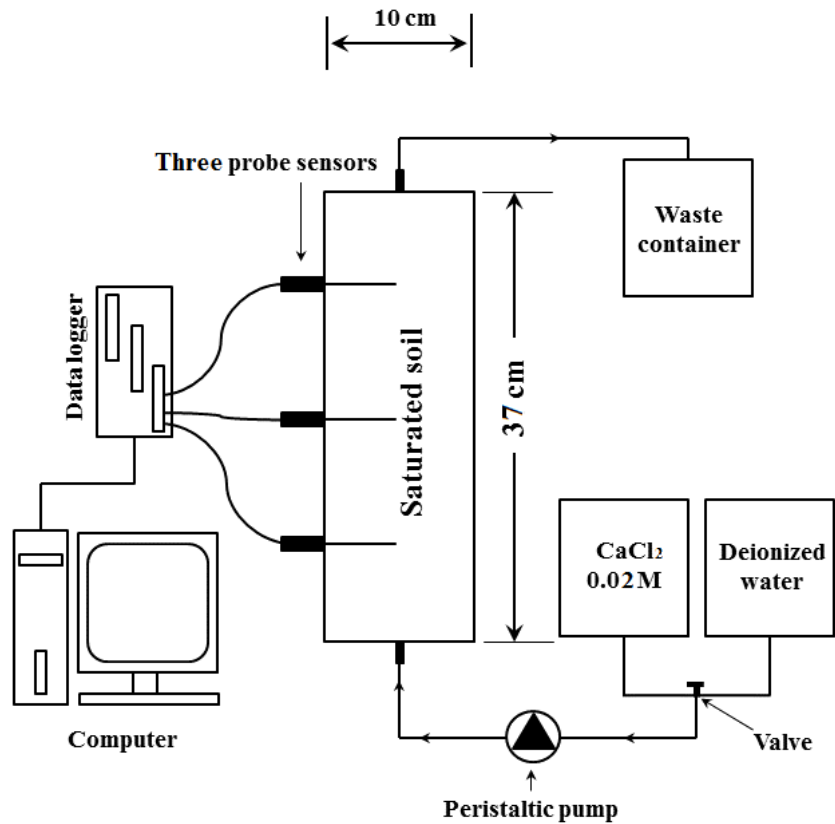


Figure 3 - Schematic of the experimental setup for the saturated column experiment.

3.6.2 Unsaturated Experiment

A schematic of the unsaturated experimental setup is shown in Figure 4. During the unsaturated experiment the peristaltic pump was connected to the top of the column and therefore the water flow direction was pointed downwards. At the top of the column a plastic distribution plate was placed to ensure complete spreading of the incoming water flux and the initial water front was homogeneous across the column. The bottom of the column was connected to a hanging column to regulate the pressure. Unit gradient flow was needed to make sure the entire column had the same water content. Since a pressure drop across the bottom filter as a result of possible clogging was likely and the magnitude of this pressure drop was difficult to predict, unit gradient flow was achieved by gradually decreasing the bottom pressure head (Toride et al., 2003). This was done by setting the water flux at the top to a constant value which coincided with the desired water content and then adjusting the height of the hanging column. The starting height was level with the bottom of the column. Each time the bottom pressure was lowered the water flow was given enough time to

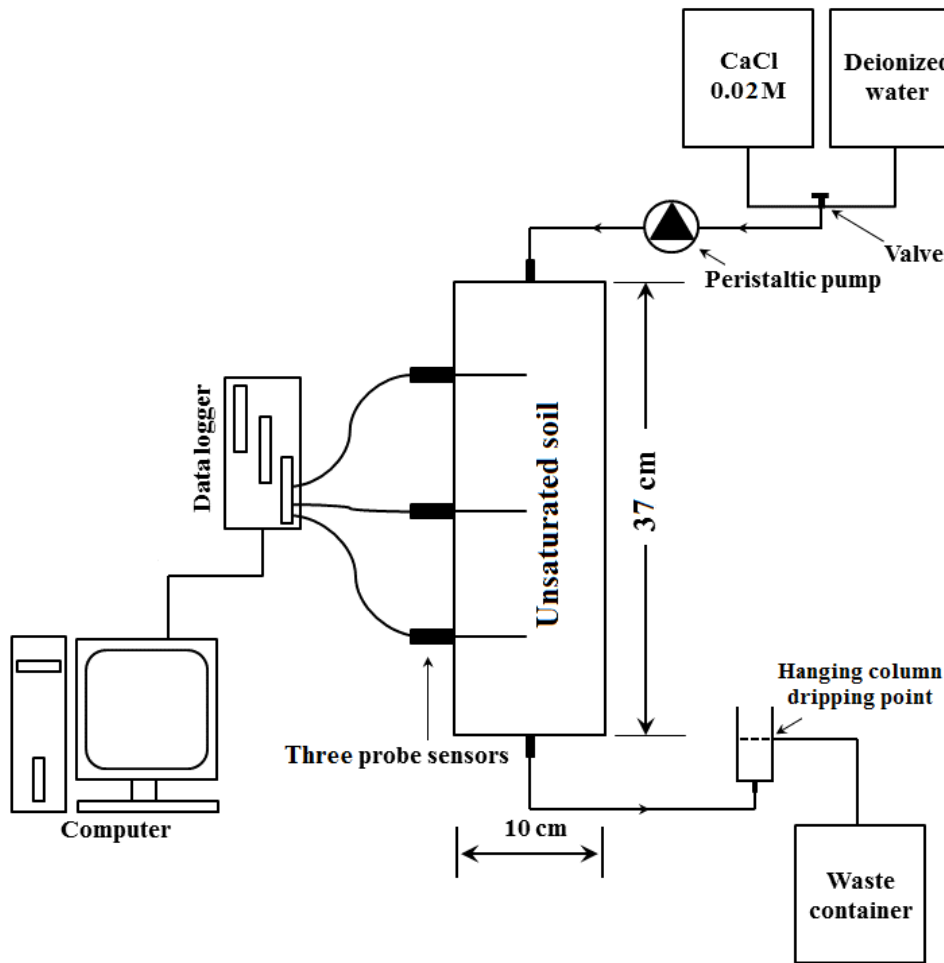


Figure 4 - Schematic of the experimental setup for the unsaturated column experiment.

reach equilibrium before lowering the bottom pressure again. To minimize hysteresis effects, the column was saturated completely before each experiment and the bottom pressure was never increased by moving the drip point of the hanging column upwards. It was only moved downwards. Ultimately, unit gradient flow was achieved and the salt tracer pulse could be injected in the same manner as during the saturated experiment.

3.7 Permittivity Measurements as a Proxy for Concentration

Whilst executing the unsaturated experiments it became apparent that the EC-meters had stopped working properly in unsaturated conditions. A possible explanation for this is that the electrodes in the 5TE sensors were separated by bubbles of air, which prevented the electrical current from the cathode from reaching the anode. This resulted in electrical conductivity data which was unusable for plotting the break through curves of the unsaturated experiments. The volumetric water content measurements, however, show an apparent decline in water content when the salt concentration in the water rises. This is due to the fact that a rise in salt concentration results in a decrease in permittivity which, in turn, is used by the sensors to calculate volumetric water content. Figure 5 shows the relation between the permittivity data and the CaCl_2 concentration as was determined in a saturated experiment with accurate electrical conductivity data. The relation shows that the decline in permittivity is linearly related to the increase in CaCl_2 concentration. However, this relation only holds for the rising limb of the BTCs. This meant that the permittivity data could be used as a proxy to plot the rising limbs of the breakthrough curves in the unsaturated experiments and the dispersivity could be determined.

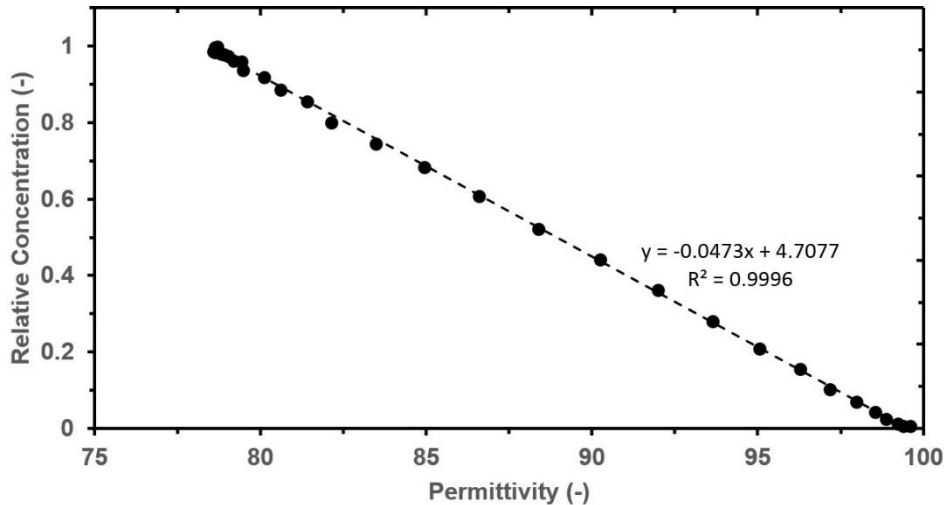


Figure 5- Relation between measured concentration, relative to the tracer solute concentration, and measured permittivity in a saturated experiment. Only the rising limb of the BTC is shown. Note that the unit for permittivity is a dimensionless non-SI unit defined by the supplier of the 5TE sensors (Decagon).

3.8 Parameter Estimation

To analyze the BTCs that were obtained during the column experiments and determine the corresponding dispersivity values, STANMOD was used. STANMOD is a computer software package that includes several separate codes for evaluating solute transport in soils and groundwater using analytical solutions of the ADE (Van Genuchten et al., 2012). The code that was used to determine the dispersivity values in this study is the inverse model of the CXTFIT2 code. Because a tracer was used for the experiments, and there was no adsorption or decay, the only parameters that were estimated were the dispersion coefficient and the pore flow velocity, where the pore flow velocity measurements were used as an initial estimate for the parameter estimation. Fitting the pore flow velocity was done to prevent any small inconsistencies in the water content throughout the column to have a negative effect on the solution of the inverse ADE.

4 Results and Discussion

4.1 Unsaturated Water Flow

Figure 6 presents the θ values for the two unsaturated column experiments at the three measurement depths along the column. The values for θ are approximately 0.13 for the first experiment and 0.15 for the second experiment. Because of the difficulty in fixing the bottom pressure at a completely accurate value, there is a small variability in the saturation values at the three measurement locations. The Darcy water fluxes for the experiments were 340 cm d^{-1} and 619 cm d^{-1} , respectively.

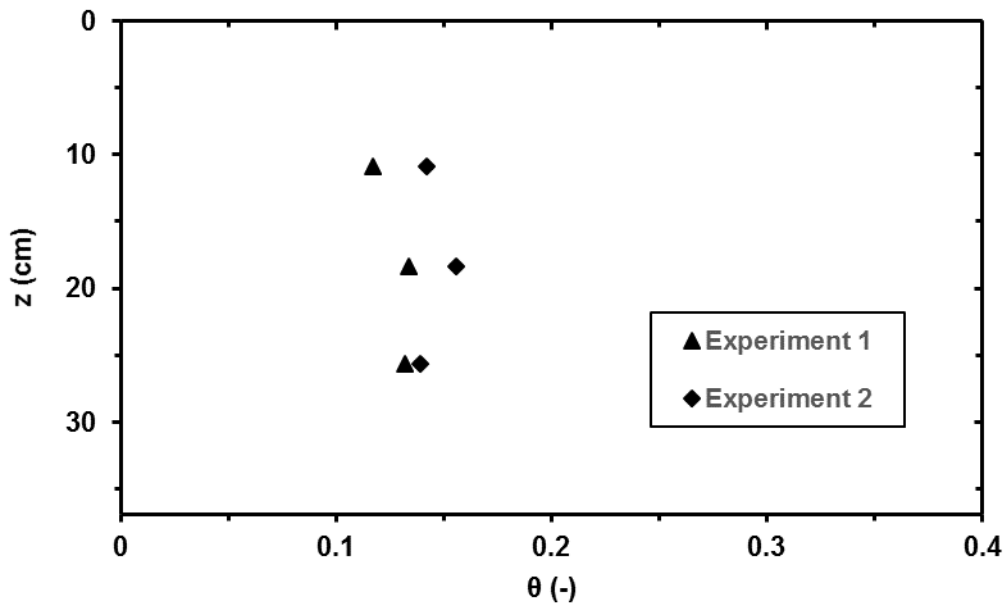


Figure 6 - Graph of volumetric water content, θ , profile during unit-gradient flow for both unsaturated experiments.

The bottom suction was approximately -50 cm for both experiments (not including a possible pressure drop through the bottom filter).

4.2 Breakthrough Curves and Parameter Estimation

BTCs have been measured during two saturated and two corresponding unsaturated experiments. All BTCs have been fitted with the inverse ADE solution of CXTFIT2 separately. Furthermore, for each experiment a one single CXTFIT2 approximation has been made using the data of all three measuring positions. These measured BTCs and the corresponding fitted curves by CXTFIT2 are shown in Figure 7 for both saturated experiments. Dimensionless concentration is plotted against time for all three measuring positions.

Analytical solutions of the ADE were fitted to the observed BTCs to determine ν and D and ultimately determine α . Table 1 shows all parameters that were obtained by using CXTFIT2. These parameters include ν , D , and r^2 that were estimated using numerical solutions of the ADE for each individual BTC as well as all BTCs per experiment. Furthermore, α has been calculated for each set of estimated parameters. Considering the estimated values for ν , a mean pore radius, L , of 0.501 mm and a D_e value of $1.19 \times 10^{-9} \text{ m}^2 \text{ s}^{-1}$, the Peclet number ranges from 13.0 to 32.1. Therefore, α has been calculated according to equation (6).

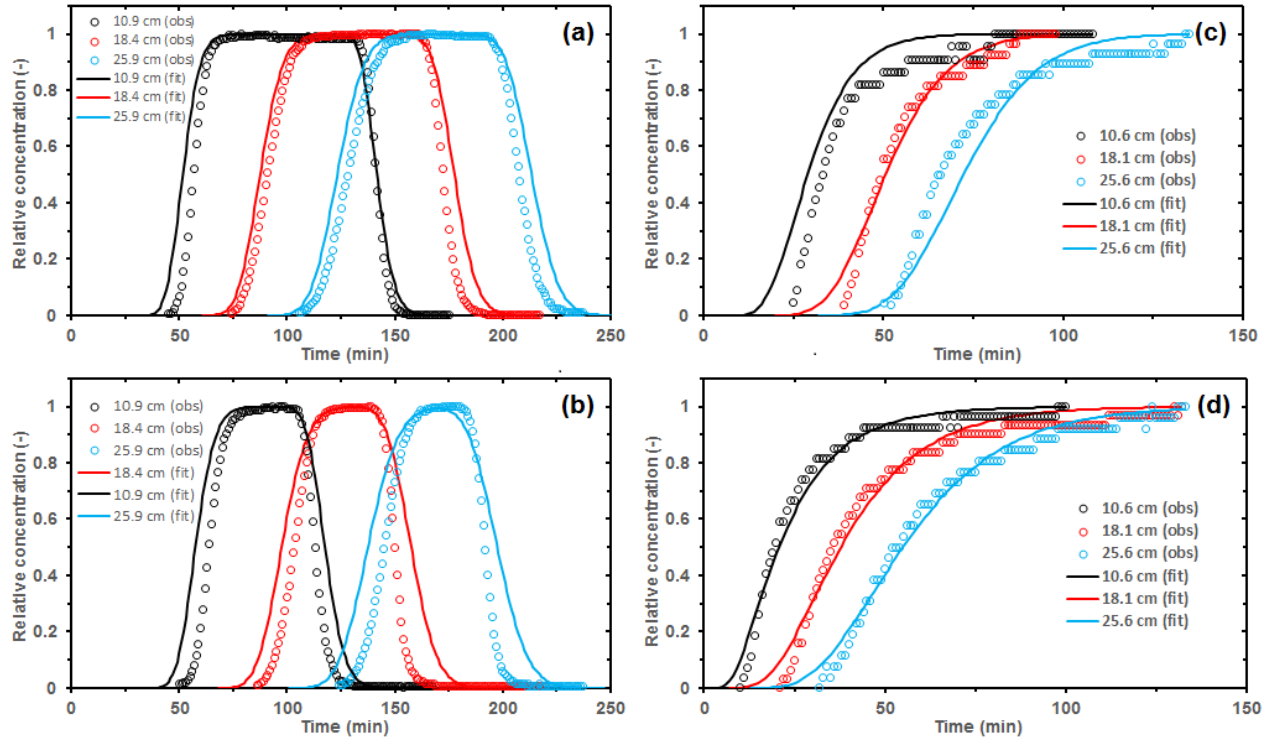


Figure 7 - Observed and fitted breakthrough curves at all three measured depths with concentrations expressed relative to the injected concentration: (a) experiment 1, saturated flow ($\theta = 0.33$), (b) experiment 2, saturated flow ($\theta = 0.34$), (c) experiment 2, unsaturated flow ($\theta = 0.13$), (d) experiment 2, unsaturated flow ($\theta = 0.15$).

Table 1 - Advection-dispersion equation (ADE) parameter estimations obtained from the breakthrough curves for saturated and unsaturated flow conditions in both experiments. The parameters are estimated for each individual breakthrough curve and for all breakthrough curves per experiment. Note that the distance from the inlet to the sensors, z , was slightly different during the saturated and unsaturated experiments.

Experiment 1						Experiment 2					
Saturated	z	ν	D	α	r^2	Saturated	z	ν	D	α	r^2
q (cm d ⁻¹)	cm	cm d ⁻¹	cm ² d ⁻¹	cm		q (cm d ⁻¹)	cm	cm d ⁻¹	cm ² d ⁻¹	cm	
87	10.9	289	27	0.089	0.9771	97	10.9	266	27	0.102	0.9381
	18.4	305	24	0.080	0.9651		18.4	274	24	0.087	0.9186
	25.65	301	15	0.053	0.9659		25.65	268	17	0.065	0.9257
	all depths	302	24	0.080	0.9583		all depths	271	22	0.082	0.9028
Unsaturated						Unsaturated					
q (cm d ⁻¹)						q (cm d ⁻¹)					
45	10.85	435	236	0.543	0.9606	65	10.85	660	1178	1.786	0.9794
	18.1	499	253	0.509	0.9741		18.1	619	1305	2.107	0.9782
	25.6	523	409	0.782	0.9724		25.6	619	1263	2.040	0.9861
	all depths	498	315	0.633	0.9137		all depths	622	1254	2.016	0.9920

Analysis of the measured BTCs of both saturated experiments showed that the total solute mass that was measured by the electrical conductivity sensors was lower than the total solute mass that was injected into the column. The difference in measured mass was larger in the second experiment than in the first experiment. Since a tracer was used, the measured mass should be the same as the injected mass as there is no adsorption or decay. A physical explanation for this has not been found, so decrease in measured solute mass along the column is probably a result of measurement errors. These errors are most likely the cause of the discrepancy between the measured BTCs and the fitted BTCs. This conclusion is substantiated by the observation that the discrepancy is larger in the data of the second experiment, which had a larger measurement error. The consequences for the accuracy of the estimated parameters are negative. Furthermore, in order to fit curves through the measured BTCs, the distance between the measurement locations must be equal. This was not the case, as the distances were 7.5 cm and 7.25 cm, respectively. This has probably also caused some inaccuracy of the fitted BTCs. However, the significance of the errors is relatively small and therefore conclusions can still be drawn from the data.

Table 1 shows that both unsaturated experiments resulted in dispersivity values that are much higher than the dispersivity values resulting from the saturated experiments. The dispersivity in both saturated experiments is approximately 0.080 cm, where the dispersivity values in the two unsaturated experiments are approximately 0.6 cm and 2.0 cm, respectively.

The dispersivity, α , has been plotted as a function of volumetric water content in Figure 8 for saturated and unsaturated conditions in both experiments.

As can be seen in Figure 8, these results do not suffice to state a clear relation between saturation and dispersivity. To be able to define a clear relation between saturation and dispersivity, more data points are needed from which a clear trend is visible. However, the results do show a clear difference in the magnitude of dispersivity between saturated and unsaturated flow conditions. Larger dispersivity values in unsaturated soils match expectations, because dispersion is caused by pore-scale bifurcations of groundwater flow paths. These bifurcations will occur more

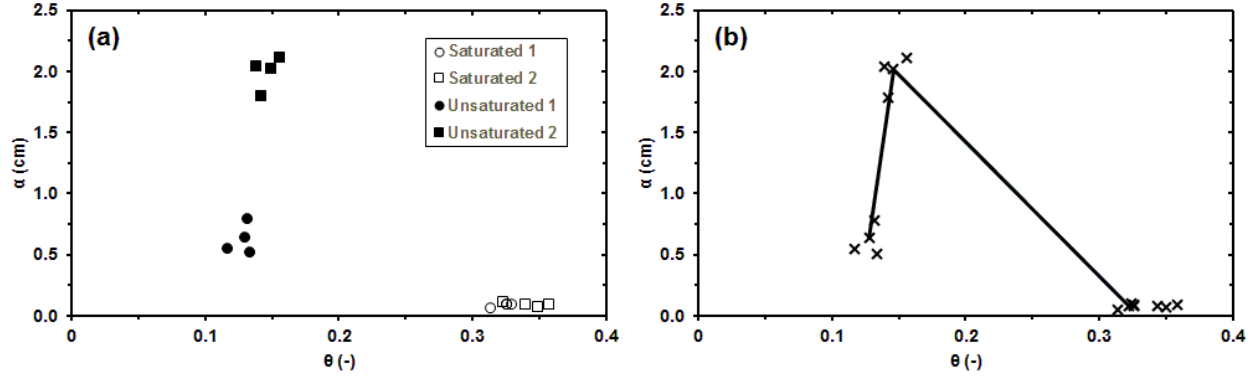


Figure 8 - Dispersivity, α , as a function of volumetric water content, θ , for saturated and unsaturated conditions in both experiments: (a) all experiments are marked separately, (b) relationship between dispersivity and saturation for all data.

frequently when there is more air entrapped in the soil, blocking potential flow paths for the groundwater. The dispersivity is larger by approximately an order of magnitude in unsaturated flow conditions than in saturated flow conditions. Earlier studies have found relationships where the dispersivity keeps increasing with decreasing saturation (De Smedt and Wieringa, 1984; Maraqa et al., 1997; Padilla et al., 1999; Kanzari et al., 2015). These relationships were expressed by equations in the form of

$$\alpha = x\theta^y \quad (13)$$

where x and y are empirically determined variables.

However, the relationship between saturation and dispersivity is, most likely more complex than can be described with an equation in the form of equation (13), since a nonmonotonic relationship has been found in laboratory experiment by Toride et al. (2003) and in a pore-network model by Raouf and Hassanizadeh (2013). They found that the maximum dispersivity values coincide with an intermediate saturation value.

In unsaturated conditions the large variability in pore-flow velocities along various flow paths is relatively high. Some saturated domains in the soil become (partially) isolated from the other fast-flowing pores and are considered to contain immobile water. Under such conditions the pore-flow velocity may vary too much to be described accurately by the ADE and a mobile-immobile model (MIM) may be needed for accurately describing the solute transport.

A MIM takes into account the large variations in pore-water velocity and the associated immobile pore-water domains. Solutes may be exchanged between the immobile pore-water and mobile pore-water through diffusion (De Smedt and Wieringa, 1979). When using a MIM to describe solute transport, the resulting dispersivity will be lower than when using an ADE model because part of the spreading of solutes is caused by mass transfer between mobile and immobile domains. This was also observed by Toride et al. (2003) as well as Raouf and Hassanizadeh (2013). However, application of a MIM in this research has not yielded any improved fitting results and are therefore not reported.

A possible explanation for this is that there were, in fact, few immobile water zones in the column during the experiments. Another explanation is that the sensor measurements were insufficiently accurate to be able to distinguish mobile-immobile transferring of solutes from solute dispersion.

Because the BTCs for the unsaturated experiments were reconstructed with permittivity measurements, there is no data on the falling limbs of these BTCs. This prevents detection of any possible tailing that could have been caused by diffusion of solute to immobile water pockets in the soil. Diffusion to immobile water would only show up as tailing in the falling limb since it is only a retarding factor with regards to solute transport. It is possible that if the falling limb data had been available, the ADE fits would have been less accurate (smaller r^2) because of the tailing caused by immobile water domains.

5 Conclusions

Two sets of experiments were conducted in a laboratory soil column. Each set of experiments consisted of solute displacement under saturated and unsaturated conditions in a soil column packed with very well-sorted coarse sand. The unsaturated experiments were conducted in a near unit-gradient flow regime, approaching a constant degree of saturation across the entire soil column. A 0.02M CaCl_2 tracer pulse was applied. The solute concentrations were measured with electrical conductivity sensors at three depths along the packed soil column. The resulting breakthrough curves were analyzed using the CXTFIT2 code, which estimated transport parameters for the advection-dispersion equation. The transport parameters were then compared to determine the relationship between saturation and dispersivity.

In both sets of experiments, the dispersivity values were much higher than in the saturated experiments. In unsaturated conditions the obtained values were approximately 0.6 cm and 2.0 cm, respectively, as opposed to the values of approximately 0.08 cm in both saturated experiments. The results show a clear dependence of dispersivity on soil water content. However, a clear relationship cannot be determined based on the results.

Previous studies have shown that the ADE often does not suffice to describe solute transport in unsaturated conditions completely accurately, because of the large variety in pore-flow velocities. These variations in pore-flow velocity can cause pore-water domains of the soil to become immobile, in which case the solute transport can best be described by a mobile-immobile model.

Because of erroneous concentration data from the unsaturated experiments, only the rising limbs of the breakthrough curves could be constructed and any potential tailing in the falling limb cannot be observed or discussed.

All results that have been discussed apply to well sorted homogeneous nonaggregated soils. Part of the difficulty of defining the relationship between soil water content and dispersivity is the variation in soil types. Every research project that is carried out has different boundary conditions which makes it difficult to build a database of experimental data to base an accurate relationship

between soil water content and dispersivity on. Applying the relationships in the field is even more difficult. In nature, soils are often heterogeneous, aggregated soils, disturbed by bioturbation and human activities (e.g. ploughing). These inconsistencies all influence dispersivity. Therefore, there is still much room for research to improve the understanding of the relationship between soil water content and dispersivity.

6 References

- Bear, J. 1972. Dynamics of fluids in porous media. p.579–663.
- Beven, K.J., Henderson, D.E., Reeves, A.D., 1993. Dispersion parameters for undisturbed partially saturated soil. *Journal of Hydrology*, Vol. 143, p. 19-43.
- Bolt, G.H., 1979. Movement of solutes in soil: Principles of adsorption/exchange chromatography. *Developments in Soil Science*, Vol. 5, p. 285-348.
- Bunsri, T., Sivakumar, M., Hagare, D., 2008. Influence of Dispersion on Transport of Tracer through Unsaturated Porous Media. *Journal of Applied Fluid Mechanics*, Vol. 1, No. 2, p. 37-44.
- Celia, M.A., Bouloutas, E.T., 1990. A General Mass-Conservative Numerical Solution for the Unsaturated Flow Equation. *Water Resources Research*, Vol. 26, p. 1483-1496.
- De Smedt, F., Wieringa, P.J., 1979. Mass Transfer in Porous Media with Immobile Water. *Journal of Hydrology*, Vol. 41, p. 59-67.
- De Smedt, F., Wieringa, P.J., 1984. Solute Transfer Through Columns of Glass Beads. *Water Resources Research*, Vol. 20, No. 2, p. 225-232.
- Folk, R.L., Ward, W.C., 1957. Brazos River bar: a study in the significance of grain size parameters. *Journal of Sedimentary Petrology*, Vol. 62, p. 3-26.
- Fried, J.J., Combarous, M.A. 1971. Dispersion in porous media. *Advances in Hydroscience*, Vol. 7, p. 169-282.
- Haga, D., Niibori, J., Chida, T., 1999. Hydrodynamic dispersion and mass transfer in unsaturated flow. *Water Resources Research*, Vol. 35, no. 4, p. 1065-1077.
- Kanzari, S., Hachicha, M., Bouhlila, R., 2015. Laboratory Method for Estimating Solute Transport Parameters of Unsaturated Soils. *American Journal of Geophysics, Geochemistry and Geosystems*, Vol. 1, No. 4, p. 151-156.
- Leij, F.J., Van Genuchten, M.Th., Yates, S.R., Russel, W.B., 1989. RETC: A Computer Program for Analyzing Soil Water Retention and Hydraulic Conductivity Data. p. 263-272. In Van Genuchten, M.Th., Leij, F.J., Lund, L.J. (ed.) *Proceedings of the International Workshop on Indirect Methods for Estimating the Hydraulic Properties of Unsaturated Soils*. University of California, Riverside, CA.

- Maciejewski, S., 1993. Numerical and experimental study of solute transport in unsaturated soils. *Journal of Contaminant Hydrology*, Vol 14, p. 193-206.
- Maraqqa, M.A., Wallace, R.B., Voice, T.C., 1997. Effects of degree of saturation on dispersivity and immobile water in sandy soil columns. *Journal of Contaminant Hydrology*, Vol. 25, p. 199-218.
- Nimmo, J.R., 2005. Unsaturated Zone Flow Processes, in Anderson, M.G., and Bear, J., eds., *Encyclopedia of Hydrological Sciences: Part 13--Groundwater: Chichester, UK, Wiley*, Vol. 4, p. 2299-2322.
- Padilla, I.Y., Jim Yeh, T.C., Conklin, M.H., 1999. The effect of water content on solute transport in unsaturated porous media. *Water Resources Research*, Vol. 35, No. 11, p. 3303-3313.
- Perret, J., Prasher, S.O., Kantzas, A., Hamilton, K., Langford, C., 2000. Preferential solute flow in intact soil columns measured by SPECT scanning. *Soil Science Society of America Journal*, Vol. 64 No. 2, p. 469-477.
- Raouf, A., Hassanizadeh, S.M., 2013. Saturation-dependent solute dispersivity in porous media: Pore-scale processes. *Water Resources Research*, Vol. 49, p. 1943-1951.
- Reynolds, W.D., Elrick, D.E., Youngs, E.G., Booltink, H.W.G., Bouma, J., 2002. Saturated and field-saturated water flow parameters. *Methods of soil analysis*, Vol. 4, p. 804-808.
- Rhoades, J.D., Manteghi, N.A., Shouse, P.J., Alves, W.J., 1989. Soil electrical conductivity and soil salinity: new formulations and calibrations. *Soil Science Society of America Journal*, Vol. 53, p. 433-439.
- Ribeiro, A.C.F., Barros, M.C.F., Teles, A.S.N., Valente A.J.M., Lobo, V.M.M., Sobral, A.J.F.N., Estes, M.A., 2008. Diffusion coefficients and electrical conductivities for calcium chloride aqueous solutions at 298.15 K and 310.15 K. *Electrochimica Acta*, Vol. 54, p. 192-196.
- Schelle, H., Iden, S.C., Peters, A., Durner, W., 2010. Analysis of the Agreement of Soil Hydraulic Properties Obtained from Multistep-Outflow and Evaporation Methods. *Vadose Zone Journal*, Vol. 9, p. 1080-1091.
- Šimůnek, J., Jacques, D., Langergraber, G., Bradford, S. A., Šejna, M., Van Genuchten, M. Th., 2013. Numerical Modeling of Contaminant Transport Using HYDRUS and its Specialized Modules. *Journal of the Indian Institute of Science*, Vol. 93, No. 2.

- Šimůnek, J., Šejna, M., Saito, H., Sakai, M., Van Genuchten, M. Th., 2012. The HYDRUS-1D Software Package for Simulating the One-Dimensional Movement of Water, Heat, and Multiple Solutes in Variably-Saturated Media. University of California-Riverside Research Reports, Vol. 3, p. 1-240.
- Toride, N., Inoue, M., Leij, F.J., 2003. Hydrodynamic Dispersion in an Unsaturated Dune Sand. Soil Science Society of America Journal, Vol. 67, p. 703-712.
- Van Genuchten, M. Th., 1980. A Closed-form equation for predicting the Hydraulic Conductivity of Unsaturated Soils. Soil Science Society of America Journal, Vol. 44, p. 892-898.
- Van Genuchten, M. Th., J.C. Parker, 1984. Boundary conditions for displacement experiments through short laboratory soil columns. Soil Science Society of America Journal, Vol. 48, p.703-708.
- Van Genuchten, M.Th., Šimůnek, J., Leij, F.J., Toride, N., Šejna, M., 2012. STANMOD: Model Use, Calibration, and Validation. American Society of Agricultural and Biological Engineers, Vol. 55(4), p. 1353-1366.

Appendices

Appendix A

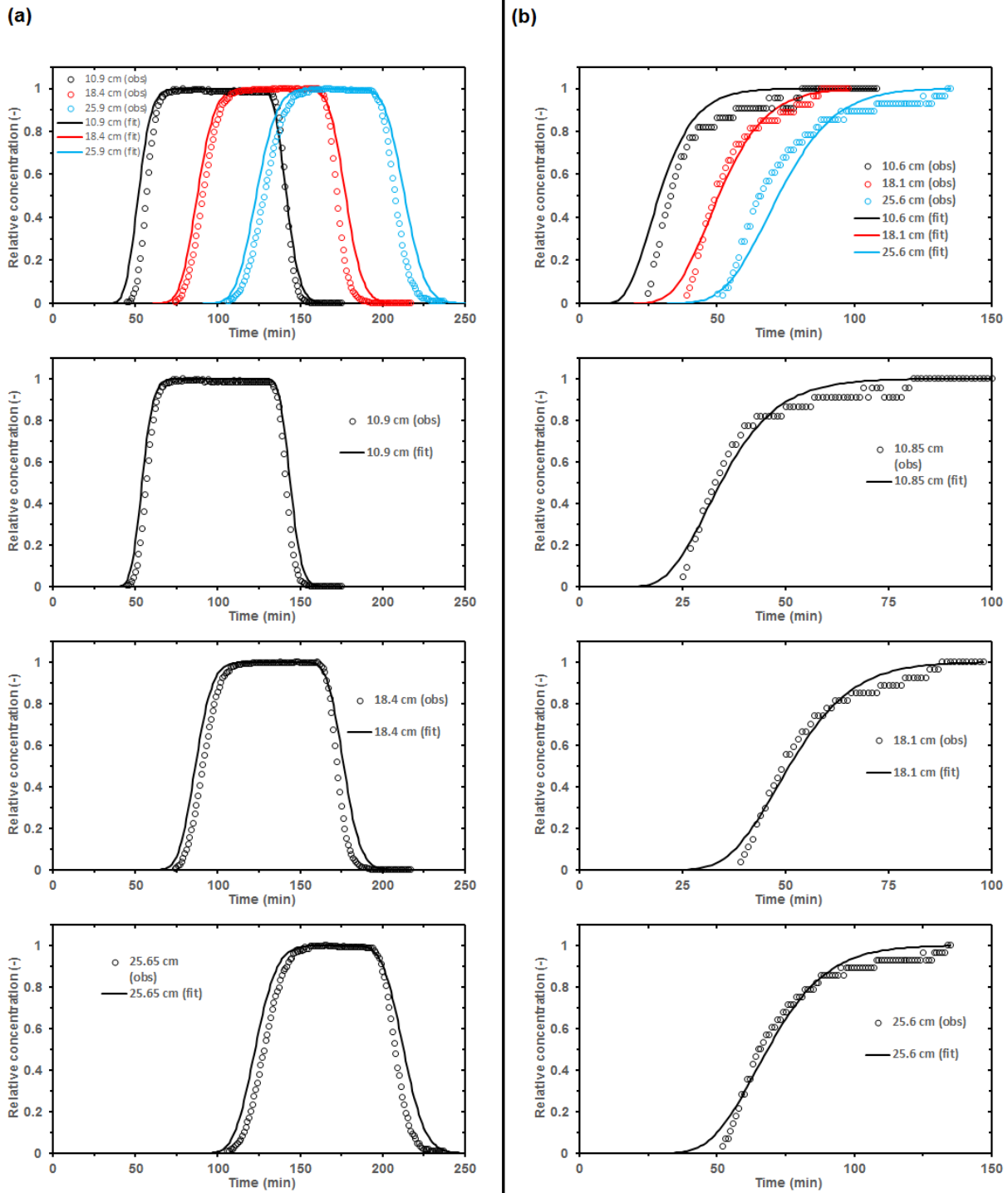


Figure 9 – All breakthrough curves of the first experiment plotted together and separate: (a) saturated and (b) unsaturated.

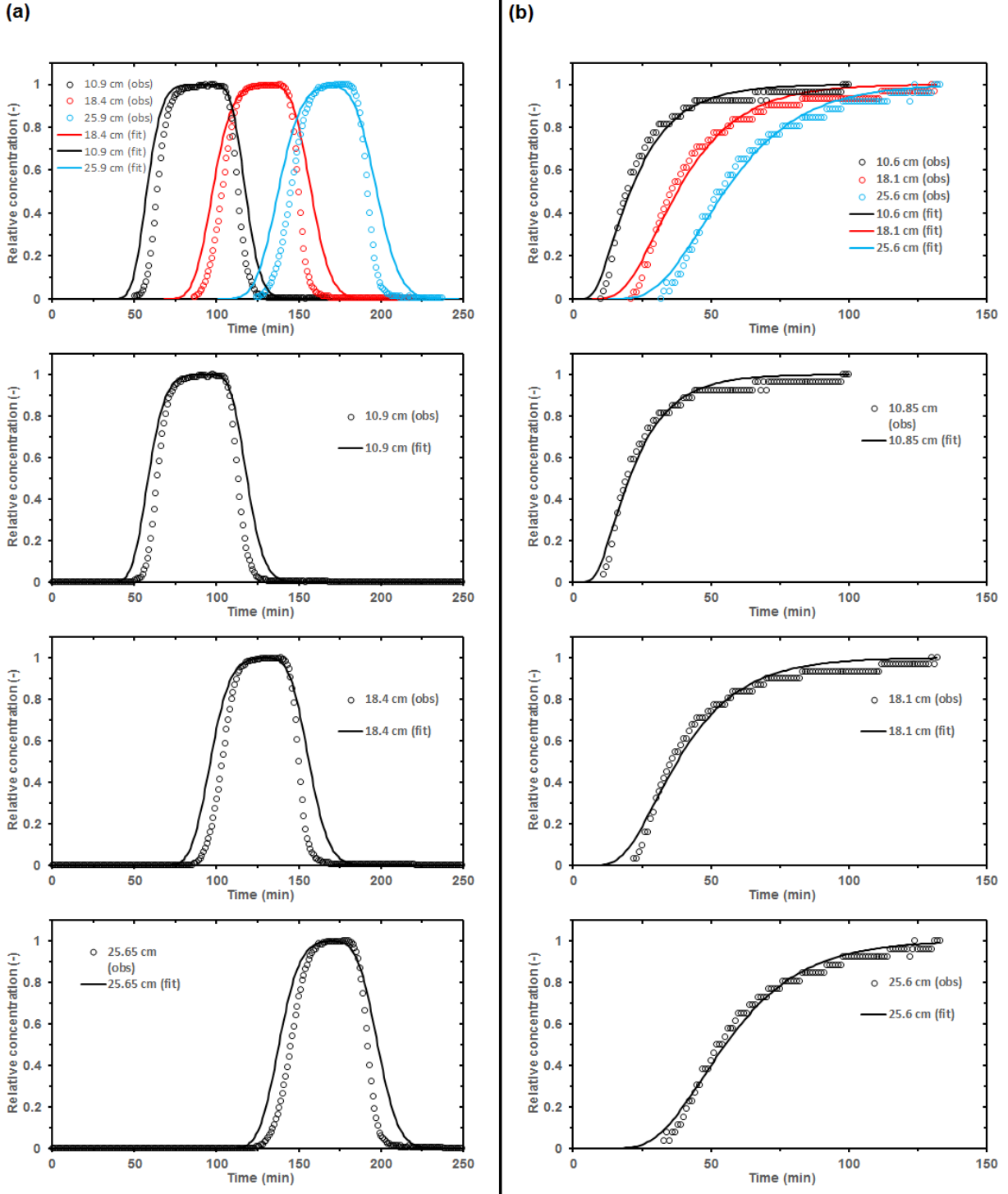


Figure 10- All breakthrough curves of the second experiment plotted together and separate: (a) saturated and (b) unsaturated.

Appendix B

Table 2 – Soil column measurements.

Length	36.65 cm
Diameter	9.5 cm
Cross sectional area	70.9 cm²
Volume	2598 cm³

Table 3 – Packed soil column data for both experiments.

	Experiment 1	Experiment 2
Total mass	6105 g	5985 g
Empty mass	1685 g	1700 g
Soil mass	4420 g	4260 g
Bulk density	1.701 g/cm³	1.629 g/cm³
Pore volume	930 cm³	1001 cm³
Porosity	0.36	0.38